

High Performance Resin Formulations with Ozone-Pretreated Corn Cob Lignin and Lysine

Sandip Singh[†], Thomas Binder[†], Erik Hagberg[‡], Bala Subramaniam^{†, #*}

[†] Center for Environmentally Beneficial Catalysis, University of Kansas, KS 66047, USA

[‡] Archer Daniels Midland Company, Decatur, IL, 62526, USA

[#] Department of Chemical and Petroleum Engineering, University of Kansas, Lawrence, KS 66045, USA

*Corresponding author: bsubramaniam@ku.edu

ABSTRACT

Non-toxic resins formulated with renewable components have been receiving increased attention as sustainable alternatives to petroleum-based resins. In this work, we demonstrate a new class of lignin-amino acid (LA) resins, formulated with non-toxic components that are abundant and can be renewably sourced from field leftovers (corn cobs) and lysine (from bio-based sugars). NMR (¹H, ³¹P, ¹³C-¹H HSQC, ¹⁵N-¹H HSQC, and ¹⁵N-¹H HMBC), FTIR, thermogravimetric, gel permeation chromatography and elemental analyses provide insights into the physicochemical properties of the resins, including the presence of LA linkages such as C-N cross linking. The LA resin creates strong bonds between pieces of wood, metals (aluminum and stainless steel) and plastics. Internal bond strengths (IBS) of balsa wood and medium density fiberboard specimens glued with LA resins, measured using an Instron instrument, were comparable to those bonded with commercial polyurethane (PU) and polyvinyl acetate (PVAc) resins. Resins prepared with ozone-pretreated lignin have significantly larger molar masses and display increased bond strengths with glued substrates as inferred from IBS measurements. This is attributed to the creation of reactive oxygen-based functionalities in the lignin upon ozone pretreatment. Lignin-amino acid resins thus show promise as a feasible and sustainable alternative to petroleum-based resins.

KEYWORDS: Corn cob lignin, acetosolv extraction, ozone treated lignin, lysine, lignin-amino acid resins, tensile strength.

INTRODUCTION

Currently, petroleum-derived chemicals are used to synthesize a variety of resins used as adhesives. Phenol-formaldehyde (PF) resin is one such example that is predominantly used in wood-based industrial products, including wood panels, plywood, laminated veneer lumber and oriented strand board.^{1, 2} PF resins account for more than half (~54%) of wood resin applications globally.² Both phenol and formaldehyde are derived predominantly from petroleum sources. According to the World Health Organization (WHO) and the United States Occupational Safety and Health Administration (OSHA), the emissions of these chemicals cause several health-related issues, including mutagenic, carcinogenic and reprotoxic effects.^{3, 4} Thus, non-toxic and sustainable resin replacements are needed that are cost effective and either match or surpass the functional performance of PF resins.

In the United States, approximately 587 million dry tons of lignocellulosic biomass can be generated, which includes crop wastes and energy crops.⁵ Lignin accounts for 15-30 wt.% of lignocellulosic biomass.⁶ Lignin is a major byproduct of the pulp and paper industry, consisting of a plurality of C-O-C and C-C linkages among the constituent aromatic structures with a high molecular weight.⁷ Lignin has been used primarily as a boiler fuel to generate heat. However, significantly more value can be created if lignin is used as feedstock for producing chemicals and materials such as carbon fibers, resins and the like,⁸ harnessing the aromatic backbone and the hydroxyl groups [primary (1°), secondary (2°) and phenolic (Ph-OH)].⁸⁻¹⁰

An example of lignin valorization is its use as an either full or partial phenol replacement in PF adhesives.^{11, 12} Suspensions of water and lignin, including milled wood lignin (MWL), formaldehyde-protected lignin (FPL), acetone-protected lignin (KPL), deep eutectic solvent-extracted lignin (DESL), kraft lignin (KL) and dioxane-HCl lignin (DL), have been reported as adhesives on wood veneers.¹³ Substitution of phenol by Kraft lignin (up to 50%) and soda lignin (up to 90%) in PF resins has also been reported.^{14, 15} Preprocessing of lignins by phenolation, glyoxalation or methylolation, has been employed for making lignin-based resins.^{14, 16}

Ozonation is a catalyst-free technique that is widely used in the pulping sector to bleach generated wastewater.¹⁷ Ozone generation technique uses either dry air or oxygen, and ozone production is widely understood at all industrial levels. Ozone has a short half-life, and the

residual O₃ from experiments can be readily and safely degraded to oxygen.¹⁸ As a result, ozonation is a clean procedure that requires no additional steps for reagent separation. Ozone is a very reactive and strong oxidant that has been used to oxyfunctionalize lignin (for example, aldehyde, quinones, ketone, and carboxylic acid groups) in mild circumstances without the use of catalysts.¹⁹

Reactive prepolymers have been synthesized by grafting aromatic aldehydes such as vanillin and 4-hydroxybenzaldehyde onto ozonized lignin.²⁰ Epoxy resins were formulated with ozonized Kraft lignin using glycerol polyglycidyl ether (GPE) in an alkaline solution. Such resins, prepared with up to 80 wt.% ozonized lignin, displayed good tensile strength.²¹ A lignin-based vitrimer was synthesized by combining ozonized Kraft lignin and sebacic acid with a zinc catalyst. The increased content of ozonized lignin in the adhesives resulted in improved tensile strength due to the creation of a densified crosslink network.²² In yet another study, ozonized lignin was combined with polyethylene glycol diglycidyl ether, bisphenol A diglycidyl ether and triethylene tetramine to create epoxy resins. However, the tensile strength of such resins is unaffected when compared to those made with unozoneized lignin.²³ Ozone-treated Kraft lignin has been utilized to produce polyurethane resins with high tensile strength, attributed to the presence of active hydroxyl groups.²⁴ The oxidative process partially converted the Kraft lignin into quinones that were subsequently used to produce the resins. However, these resins displayed lower tensile strength than formaldehyde-based resins due to fewer bonds formed between the phenolic alcohol and aldehyde groups.²⁵ In another investigation, lignin oxidation was facilitated by laccase, and the oxidized lignin was used to produce lignin-based formaldehyde (LF) resins.²⁶ Different types of lignin as polyol sources were used to develop polyurethane products for adhesives and coating applications.²⁷

Replacement of formaldehyde in PF with safer and less toxic substituents has long been sought.²⁸ Chemicals such as citric acid, terephthalaldehyde, furfural, succinic anhydride, soy protein matrix, hydroxymethyl furfural or glyoxal have been reported as either partial or full substituents for formaldehyde in PF-resins.^{29, 30} However, these alternate formulations are plagued by issues such as corrosion and long adhesion time, and have not gained commercial

acceptance.³¹ It has been reported that amino acids and their derivatives are good corrosion inhibitors due to the presence of –OH, –COOH, and NH₂ groups.^{32, 33}

An amino acid such as lysine shows promise in this regard as a bioactive molecule with negligible, if any, toxicity. Lysine and urethane-based tissue adhesives have been synthesized and applied for mastectomy.^{34, 35} Lysine has also been added as a curing agent in soy-based wood adhesives to enhance the mechanical strength by forming strong chemical bonds between wood surface and amino acid groups.³⁶ For example, poly-lysine has been used for tissue and cell adhesion,³⁷ immunocytochemical staining,³⁸ and as a coating to enhance the adhesion and maturation of cortical neuron cultures *in vitro*.³⁹

In this work, we synthesized lignin-amino acid (LA) resins, utilizing either acetosolv lignin, or acetosolv lignin functionalized by ozone pretreatment, or combinations thereof. The lignin is obtained from corn cobs, a field leftover, while the amino acid (lysine) is sourced from fermentation of bio-based sugars with ammonium compounds.⁴⁰ The emerging hydrogen hubs will produce carbon-free oxygen as coproduct, from which ozone can be made with renewable electricity. The LA resins were thus formulated using non-toxic feedstocks and benign reagents in aqueous media. The physicochemical and structural properties of these resins were characterized by a complement of analytical techniques including nuclear magnetic resonance (NMR) spectroscopy (¹H, ³¹P, ¹³C-¹H HSQC, and ¹⁵N-¹H HMBC), Fourier transform infrared (FTIR) spectroscopy, thermogravimetric analysis (TGA), gel permeation chromatography (GPC) and elemental analysis. The ability of the synthesized resins to bond pieces of wood, metals and plastics were tested using shear test and an electromechanical tester (Instron instrument) to measure the tensile strengths of the bonded materials. Benchmarking studies show that the resins synthesized with ozone-pretreated acetosolv lignin are superior to those made without ozone pretreatment. Further, for wood-based applications, the LA resins show promising performance when compared with commercial polyurethane (PU) and polyvinyl acetate (PVAc) resins.

EXPERIMENTAL

Materials

Acetosolv lignin (AL) and ozonized acetosolv lignin (OLA) were synthesized as described earlier.⁴¹ Chromium (III) acetylacetone (97%), dimethylsulfoxide-d₆ (99.5%), and sodium hydroxide (98%) were purchased from Thermo Scientific, USA. Deuterium hydroxide (99.9%, contained 0.05 wt.%, 3-(trimethylsilyl) propionic 2,2,3,3-d₄ acid, sodium salt) was purchased from Sigma Aldrich, USA. DI water (ACS reagent grade) was purchased from Lab Chem, USA. Lysine monohydrate (99%) and dimethyl formamide (HPLC grade, 99.5%) were purchased from Fisher Scientific, USA. Tetrabutyl-ammonium bromide (\geq 99.0) was purchased from Sigma Aldrich, India. All reagents were used as received. Strips of multipurpose 304 stainless steel (0.0600" thick), multipurpose 6061 aluminum (1/16" thick), balsa wood (1/8" thick), CDX grade plywood sheet (3/8" thick), medium density fiberboard sheet, (3/8" thick) and polycarbonate (1/8" thick) were purchased for McMaster-Carr, USA. Maple veneer (0.05" thick) and walnut veneer (0.05" thick) sheets were purchased from Amazon. Brass weights with hooks (2000 g each) were purchased from Fisher Scientific, USA. FTIR grade potassium bromide was purchased from Sigma, USA. Polyvinyl acetate (PVAc) resin was purchased from TRAN tow Inc. Portland Colombia, OR, USA. Polyurethane (PU) resin was purchased from Akfix, Amazon, USA. Hexamethylenetetramine (HMTA, \geq 99.5%) was purchased from Sigma Aldrich, USA.

Synthesis of Lignin-based Resin

The lignin sample (\sim 1.0 g dry weight) was taken in a high-temperature, high-pressure glass tube (38 mL, Ace Glass, Inc.). DI water (10 mL) along with 100 mg sodium hydroxide were added into the tube. The contents were stirred using a magnetic stir bar at room temperature (RT \sim 20 °C) for 1 h to solubilize and activate the lignin functionalities such as carboxylic and hydroxyl groups. Lysine (\sim 1.0 g) was then added to the mixture and stirred at RT for another 4 h. The resulting mixture was placed in an oven at 60 \pm 2 °C for two days and then allowed to cool to ambient conditions, forming a lignin-amino acid (LA) resin. In a few cases, acetosolv lignin pretreated with ozone in a spray ozonation reactor as described elsewhere⁴¹ was used to prepare the resin, termed as OLA. In addition, different ratios of acetosolv lignin (AL) and ozonized acetosolv lignin

(OAL) (9:1, 3:1, 1:1 and 1:3 wt/wt, respectively) were also used to prepare the resins. These resins were termed as AL:OAL (9:1), AL:OAL (3:1), AL:OAL (1:1) and AL:OAL (1:3), respectively. The resins were stored in an open tube in a fume hood at ambient conditions for 24 h. Thereafter, the mixture was stored in a 20 mL glass vial for further characterization. The synthesized resins using acetosolv lignin (LA), ozone-pretreated lignin (OLA) and combinations thereof were concentrated (to approximately 50% solid) on a hot plate (~100 °C, 30 min) prior to applying over the wood specimens for the Instron test.

Reactions of Lignin Model Compounds with Lysine

Lignin model compounds, including 4-hydroxy-3-methoxybenzyl alcohol, 4-hydroxy-3-methoxy acetophenone and guaiacol glyceryl ether, cumulatively representing the presence of a carbonyl group, a vacant C5 position of methoxy, and different types of hydroxyl groups [primary (1°), secondary (2°) and phenolic (Ph-OH)] were used to gain more insights into lignin and lysine bond formation by cross-linking. The reaction between these lignin model compounds and lysine, and associated work up procedures were performed following a similar procedure as explained in the preceding section.

Physicochemical Characterization

Elemental analysis. Elemental analyses of acetosolv lignin (AL), ozonized acetosolv lignin (OAL), lignin-amino acid resin (LA) and ozonized lignin-amino acid (OLA) resin were performed by the dry combustion method. Approximately 150 mg of each sample was used for analysis. A LECO CN828 carbon/nitrogen combustion analyzer was used to determine the amounts (inorganic and organic) of C and N on a weight percent basis. Prior to elemental analysis, the resin samples were dried in a vacuum oven at 120 °C for 8 h.

Thermal analysis. Thermogravimetric analysis (TGA) of lignin and resin samples were performed using a TA SDT 600 instrument. TGA analysis of the two lignin and two resin samples (~15 mg each) was done in flowing nitrogen (100 std cm³/min) with a heating rate of 10 °C/ min from 50 °C to 800 °C.

To evaluate resin curing temperatures, Differential Scanning Calorimetry (DSC) analysis was done of resin samples containing hexamethylenetetramine (HMTA) using a TA SDT 600 Instrument. The samples were prepared using a previously reported procedure.²⁵ The HMTA was used as a curing agent in the dry resin sample at a concentration of 10 wt.%. The ground sample was oven-dried at 70±2 °C for 24 h before measurement. The sample was heated at a rate of 10 °C/min from 20 to 200 °C using nitrogen and a flow rate of 50 std cm³/min.

Structural insights using Fourier Transform Infrared Spectroscopy (FTIR). A Bruker Tensor 27 FTIR Spectrometer was used to determine the functional groups in the lignin (AL, and OAL) and resin (LA and OLA) samples. Approximately 1 mg of the sample was mixed with ~99 mg IR-grade potassium bromide. The spectra were recorded from 800 to 4000 cm⁻¹ using 64 scans.

Gel Permeation Chromatography (GPC). An Agilent 1260 Infiniti GPC system was used to determine the relative molar mass distributions of the lignin and resin samples. Two columns in series, a 300 mm Polargel-M followed by a 300 mm Polargel-L, were used for molar mass analysis at 40 °C. Approximately 4 mg lignin were dissolved in 1 mL dimethyl formamide (DMF, HPLC grade) while DI water (1 mL) was used to dissolve the lignin-amino acid resin (~4 mg). DMF with 0.1 wt% tetrabutylammonium bromide (TBAB) was used as the mobile phase flowed at 1 mL/min. The column oven and RI detector temperatures were maintained at 35 °C. Poly(methyl methacrylate) standards with molar masses ranging from 680 to 327,000 Da were used as calibration standards.⁴¹

Structural insights using ¹H, ¹³C, ¹³C-¹H 2D- HSQC, ¹⁵N-¹H 2D – HMBC, and ¹⁵N-¹H HSQC correlation NMR. The ¹H, ¹³C, and ¹³C-¹H 2D- Heteronuclear Single Quantum Correlation (HSQC) and ¹⁵N-¹H 2D Heteronuclear Multiple Bond Correlation (HMBC) spectra of lysine, lignin, and resin samples were recorded using a Bruker 500 MHz instrument. The NMR samples were prepared following published procedures with minor modifications.⁴² Different amounts of each sample [listed in Table S1 (SI)] with approximately 2 mg chromium (III) acetylacetone were taken in a 2 mL transparent HPLC glass vial. The lignins were dissolved in DMSO-d₆, while D₂O was used to dissolve the lignin-amino acid resins. The mixture was sonicated under ambient

conditions for approximately 15 min to facilitate complete solubilization. The homogeneous mixture was then transferred into an NMR tube and processed for analysis.

The HMBC spectra were recorded at 500.19 MHz and 50.36 MHz for ¹H and ¹⁵N nuclei, respectively. The applied current pulse program was hmbcgpdqf. The number of scans was 64 for the two lignin samples and 128 for the resin samples. The applied receiver gain was 2050 for each sample. The acquisition time for F2 (¹H) and F1 (¹⁵N) was 0.2925 s and 0.00414 s, respectively.

The ¹⁵N-¹H HSQC spectra of lysine, LA and OLA were recorded at 599.74 MHz and 60.77 MHz for ¹H and ¹⁵N nuclei, respectively. To record the spectra, the hsqcetf3gp pulse program was applied. The 256 number of scans was applied. The applied number of receiver gain was for each sample was 1024. The acquisition time for F2 (¹H) and F1 (¹⁵N) was 0.1425 s and 0.0132 s, respectively.

Quantification of hydroxyl groups using ³¹P NMR. The types of hydroxyl groups present in the lignin and resin samples were determined by using ³¹P NMR spectroscopy with a Bruker 500 MHz instrument. Sample preparation and peak assignments were guided by published information.⁴³ In a glove box, approximately 9.6±1.15 mg sample were dissolved in anhydrous DMF (300 μ L) and a mixture of deuterated chloroform and anhydrous pyridine (325 μ L, 1:1.6 v/v). Cyclohexanol (22.0 mg/mL) as internal standard was dissolved in a mixture (100 μ L) of deuterated chloroform and anhydrous pyridine mixture (1:1.6 v/v) and added to the tube. Chromium (III) acetylacetone solution (5.0 mg/mL), as a relaxing agent, prepared in 50 μ L of a mixture of deuterated chloroform and anhydrous pyridine (1:1.6 v/v), was also added to the tube. Finally, 2-chloro-4,4,5,5-tetramethyl-1,3,2-dioxaphospholane (100 μ L), as a phosphorylating reagent, was added into the sample tube. The sample NMR tube was processed for ³¹P NMR spectroscopy studies employing the parameters provided in Table S2 (SI).

Qualitative shear test. The performance of the synthesized resins was qualitatively assessed by gluing pieces of aluminum, stainless steel, polycarbonate and wood together, and subjecting them to vertical shear by weights. Table S4 (SI) contains information about the adherent's dimensions. With the exception of wood, which was glued with 200 mg of resin, the specimens

were bonded together using ~20 mg of resin. Following drying of the glued samples by drying at 60 ± 2 °C for 2 h, the vertical shear test was done at ambient conditions.

In another test, paper was glued to wood, stainless steel, aluminum and polycarbonate specimens with the lignin resins. Table S4 (SI) contains information on paper and specimen dimensions. Approximately 50 mg of resin was used at each end of the paper. The glued specimens were dried at 60 ± 2 °C for 2 hours, followed by a vertical shear test performed at ambient conditions.

Preparation of wood specimens for tensile test. A MTS Criterion Model 43 system (50 kN) was used to benchmark the tensile strengths of the lignin-based resins (LA and OLA) with commercially obtained resins [polyurethane (PU) and polyvinyl acetate (PVAc)] when bonding wood samples including balsa wood, CDX grade plywood, medium density fiberboard, walnut veneer and maple veneer. Balsa wood, CDX grade plywood, and medium density fiberboard specimens were prepared for the Instron test using the ASTM D 2339-20 method with minor modifications, while maple and walnut veneer specimens were prepared using the ASTM D 7998-19 method. The dimensions and glued area for all samples are given in Table S6 (SI). Clips were used to hold the samples together when drying the resins in an oven at 60 ± 2 °C for 2 h. Samples of identical size and resin loading were similarly prepared with the commercial resins (PU and PVAc) to analyze comparative tensile strengths. The directions of the long grain in the balsa wood, maple veneer and walnut veneer specimens were aligned when they were glued with the lignin-amino acid resins and commercial resins. The Instron tests were carried out at a constant strain rate of 1 mm/min by applying a longitudinal load to stretch the bonded specimens. The resulting stress-strain curves and captured visual images of the tested specimens were used to interpret the mode of failure for each specimen.

RESULTS AND DISCUSSION

Physicochemical characteristics of resins

As expected, higher nitrogen contents (8.9 wt%) are observed in the resins (Figure 1A). As shown in Figure 1A, the residual mass reflected in the TGA profiles is lower in the lignin resins compared to the lignins from which they are made, attributed to the introduction of thermally

labile moieties in the resins. Note that the residual masses in the case of ozone-pretreated lignins and resins are lower compared to the non-ozonized counterparts, attributed to the increase in the oxygen content caused by ozone pretreatment [Figure S1 (SI)]. GPC spectra (Figure 1B) show that the ozone pretreatment of the acetosolv lignin (AL) largely preserves the molecular weight distribution at higher molar masses. The ozone-pretreated lignin (OAL) solution shows peaks at lower molar masses due to the formation of oligomers (Figure 1B) and the selective cleavage of the lignin-carbohydrate complexes by ozone resulting in the formation of vanillin and *p*-hydroxybenzaldehyde [Figure S11, (SI)].⁴¹ Further, the molar mass distribution in the acetosolv lignin and the resin (LA) derived from it are almost similar. This suggests that the C-N cross-linking reaction between the lignin and amino acid, confirmed by the formation of a new carbodiimide crosslink (N=C=N-bond) at 2102 cm⁻¹ in the LA and OLA resins (Figure 1C),⁴⁴ does not cause any significant shift in the molar mass distribution. The -C-N-cross-linking reaction results in the abstraction of the carbonyl group (1705 and 1737 cm⁻¹) from the acetosolv lignin and ozonized acetosolv lignin samples.⁴⁵ The slight shift in carbonyl peak of OAL is attributed to the formation of ester/carboxylic groups.⁴⁶ The interaction of amino acids with alcohol and aldehyde groups to form amine compounds is known.^{47, 48}

The resin prepared with ozone-pretreated lignin (OLA) displays significantly higher molar masses (Mw = 204.6 kDa) compared to the resin prepared without ozone pretreatment [LA, (Mw = 139.8 kDa)]. We speculate that this is due to increased lignin reactivity stemming from the formation of oxygen-containing functional groups upon ozone pretreatment.⁴⁹ Elemental analysis of the ozone-pretreated lignin confirms an increase in its oxygen content (Table S5, SI). Additional evidence of increased oxygen content in the lignin upon ozone pretreatment is provided in the following section. Further, as discussed later, the resins prepared with ozone-pretreated lignin display higher tensile strengths.

Figure 1D shows the DSC thermograms for LA and OLA resins. The curing peak temperatures of resins vary from ~146 to 180 °C, which are comparable to phenol-formaldehyde resin.²⁵ Interestingly, the OLA resin cured at lower temperatures than LA resin.

Structural insights from ^1H , ^1H - ^{13}C HSQC and ^{31}P NMR results

The ^1H NMR of resins (LA and OLA) and lignins (AL and OAL) are shown in Figures 2A, 2B and S2 (SI), respectively. The resin samples show shifts in the aliphatic signals along with the appearance of multiple new peaks. These changes are attributed to the creation of cross-linking bonds in the resins due to interactions between the lignin and lysine.⁵⁰ For example, the aldehyde proton peak present in the parent lignin at 9.75 ppm is absent in the resin [Figures 2A and S2A (SI)]. For the acetosolv lignin (AL), the disappearance of the aldehyde proton in the NMR spectra is consistent with the disappearance of the carbonyl group at 1705 cm^{-1} in the FTIR spectrum (Figure 1C). Cross-linking between amine and aldehyde groups has been reported in the generation of Schiff bases.⁵¹

The ^1H - ^{13}C Heteronuclear Single Quantum Correlation (2D-HSQC) spectra of the two lignin and two resin samples are shown in Figures 2C, 2D and S3 (SI). Barring the appearance of a few strong aliphatic signals in the two resins, the structural characteristics of the lignins and resins are comparable.^{52, 53} The primary bond found in a majority of lignins, β -aryl ether, is absent in the acetosolv lignin, consistent with earlier findings.⁵³ The occurrence of extra peaks in the aliphatic region of the resins suggests cross-linking of the amino acid with functional groups in the lignin.⁵⁴ A majority of the aromatic signals in the acetosolv lignin were preserved in the resins.⁵²

To correlate the results of the 1D and 2D NMR spectra, ^{31}P NMR spectra of the lignins and resins were also obtained (Figures 2E and 2F). This specifically allowed the identification of the various hydroxyl groups (phenolic, secondary and aliphatic hydroxy) involved in the cross-linking reaction between the amino acid and the lignins. Peak assignments for the ^{31}P NMR spectra of lignin and the resin samples were guided by previous reports.⁴³ Consistent with the removal of ~10 wt% phenolic monomers (vanillin and *p*-hydroxybenzaldehyde, in particular) following ozonolysis of the acetosolv lignin,⁴¹ the ozone-pretreated lignin shows decreases in the canonical monolignols.^{55, 56} However, the ozone-pretreated lignin shows measurable increases in the hydroxyl and carboxylic acid groups suggesting hydroxylation of both aliphatic and aromatic groups in the ozone-pretreated lignin [Figures 2E, 2F, and S4 (SI)]. The signal for carbodiimide crosslinking at 2102 cm^{-1} provides strong evidence for the cross-linking involving the aliphatic -OH groups in lignin and the -NH₂ group in the amino acid, explaining the decrease in the aliphatic

-OH groups in the resins.⁴⁴ Both the lignin resins (LA and OLA) show a decrease in G-OH (guaiacyl hydroxyl groups) and an increase in S-OH (syringyl hydroxyl groups). The number of carboxylic acid hydroxyl groups was found to be significantly higher in the LA and OLA resins compared to the lignins from which they are derived (Figure 2F). This suggests that the amine functional groups, rather than the carboxylic acid groups, in the amino acid are mainly involved in the cross-linking reactions giving rise to the carbodiimide IR signal at 2102 cm⁻¹ in the resins (Figure 1C).⁴⁷

57

To gain more insights into the cross-linking reaction and structure of lignin-amino acid resins, ¹⁵N-¹H heteronuclear multiple bond correlation (HMBC) spectra of several model formulations synthesized with lysine and lignin model compounds (4-hydroxy-3-methoxyacetophenone, 4-hydroxy-3-methoxybenzyl alcohol and glycerol glyceryl ether) were investigated. The structural inputs corresponding to the ¹⁵N-¹H HMBC correlation signals are shown in Table S3 (SI). The three ¹⁵N-¹H HMBC signals of lysine correspond to α -amino groups at 33.1/3.2 ppm and to ϵ -amino groups at 29.5/2.8 and 30.7/1.6 ppm [Figure 3A, Table S3 (SI)].⁵⁸ In most of the synthesized formulations, the ϵ -amino groups did not undergo any significant change. In contrast, changes were seen in the α -amino groups suggesting that they are reactive and instrumental in creating the C-N cross-linking products. Furthermore, Figures 3B, 3C and 3D showed signals for ¹⁵N-¹H at 93.9-95.1/1.4-1.6 ppm and 88.0/1.3-2.9 ppm, respectively, corresponding to formulations of 4-hydroxy-3-methoxybenzyl alcohol and lysine, 4-hydroxy-3-methoxyacetophenone and lysine, and glycerol glyceryl ether and lysine. These formulations are exemplary of C5-lignin, forming C-N cross condensed products due to the involvement of ϵ -amino groups.⁵⁹ The signal at 126.1/1.6 ppm in the 4-hydroxy-3-methoxyacetophenone and lysine product as well as the LA formulation may be indicative of interaction between carbonyl and amino groups (Figure 3E). Notably, the OLA resin synthesized with ozone-pretreated lignin shows an additional signal at 129.4/7.9 ppm that could be associated with new types of aromatic compounds (Figure 3F).⁶⁰

Comparison of ¹⁵N-¹H 2D-HSQC spectra of lysine (Figure 4A), LA resin (Figure 4B) and OLA (Figure 4C) resin reveals that only the OLA resin exhibits a characteristic peak at 122.7/7.3 ppm in the amide/aromatic region (Figure 4C),⁶¹ suggesting a different type of C-N/H-N linkage compared to the LA resin prepared with acetosolv lignin without ozone pretreatment.

Qualitative shear test

The durability of the lignin resins was assessed by qualitative shear test as explained in the Experimental section. Various specimens including wood-wood (W-W), polycarbonate-polycarbonate (PC-PC), aluminum-aluminum (Al-Al) and stainless steel-stainless steel (SS-SS) as well as composite W-Al, W-PC, PC-SS, and PC-Al samples were investigated. Figure 5 and Table S4 (SI) provide details on specimen dimensions and resin application areas. All specimens formed robust bonds with the lignin-amino acid resins (LA and OLA). The bonded specimens can hold a load of 2 kgs that is more than six orders of magnitude greater than the weight of the applied resin for several (> 13 so far) months without breaking (Figures 5A, 5B and 5C). Specimens glued with printed paper used to identify the specimens also show resilience during vertical shear test (Figure S5, SI).

Tensile Strength

For determining the tensile strength, various lignin resins [LA, OLA, AL:OAL (9:1), AL:OAL (3:1), AL:OAL (1:1) and AL:OAL 1:3)] were used to bond pieces of wood samples including balsa, medium density fiberboard, CDX grade plywood, walnut veneer and maple veneer samples, as explained in the Experimental section. The measured tensile strengths and failure modes were compared with the bonding performance of commercial resins such as polyvinyl acetate (PVAc) and polyurethane (PU) as benchmarks. Figures 6A and 6B depict how different specimens glued with various lignin-based resins and commercial resins were prepared for the Instron tests.

Figure 6C shows the different failure modes typically associated with bonded specimens. “Adhesive failure” occurs when the resin peels off cleanly from the bonded surface. “Substrate failure” (Figure 6D) occurs when the substrate breaks apart without either adhesive or cohesive failure occurring, indicating excellent resin adhesion to the substrate surface. Substrate “pilling” (Figure 6E) is associated with the stretching and peeling of substrate layers in the direction of the applied load with surface adhesion to the resins still intact. “Cohesive failure” (Figure 6F) occurs when the resin is still bonded to the two surfaces but is sheared off in the middle due to the applied tensile stress. The relative performances of the bonding abilities of the various resins in the range of applied tensile stresses are assessed based on the stress-strain curves of the various resin-bonded samples [Figure S6 (SI), and Table S7 (SI)] and visual images of the failure modes.

Figure 7 shows the stress-strain curves as well as visual images obtained from the Instron test of medium density fiberboard specimens glued with lignin-amino acid and commercial resins. The medium density fiberboard specimens glued with LA and AL:OAL (3:1) resins show the expected trend of increasing strain with applied stress followed by a sharp drop in the stress beyond a certain strain level. The sharp drop is indicative of cohesive failure as inferred from the visual images of these specimens at the failure stress (Figure 7B). It must be noted that the occurrences of horizontal segments in the stress-strain curves, depicting strain at constant stress, are artifacts caused by clamp slippage. Such artifacts do not however affect the accuracy of the stress value at failure. The tensile stress value at failure is calculated by normalizing the corresponding stress value with the glued surface area that is subjected to shear. The stress values at failure are then used for comparing the performances of the various adhesives. Note that medium density fiberboard specimens glued with OLA, AL:OAL (1:1), AL:OAL (1:3), commercial PVAc resin and commercial PU resin display a more gradual decline following a stress maximum (Figure 7A). This trend is characteristic of the pilling mode of failure of these specimens as also evident in their visual images post failure (Figure 7B).

Medium density fiberboard glued with OLA [Figures S8B (SI), 7B [AL:OAL (1:1)], and [S8E (SI) [AL:OAL (1:3)]] displayed the pilling mode of substrate failure. In this failure mode, the resins formed strong bonds with the adherents showing better tolerance to the applied stress compared to the adherent (Figure 8B). Clearly, using $\geq 50\%$ ozone-pretreated lignin in synthesizing the composite resins imparts better surface adhesion properties to these resins. In contrast, medium density fiberboards glued with AL:OAL composite resins prepared with $< 50\%$ OAL content [LA, AL:OAL (3:1)] undergo cohesive failure (Figure 7B). This is a clear indication that decreasing the OAL content in the composite resins weakens their bond strengths. The change in the failure mechanism with increased content of ozonized lignin in the resin suggests an opportunity for optimization aimed at maximizing the tensile strength of these resins by tuning the ozonized lignin content. The increased molecular mass (Figure 1B), increased oxygen content of ozonized lignin (Table S5, SI) and the evidence of C-N bond formation (Figures 1C, 3F and 4C) correlate with the increased tensile strength of the resins. The formation of oxygen functional groups in ozone-pretreated lignin and the resulting increased reactivity has also been reported

by other researchers.⁴⁹ The OAL resins display a variety of functional groups (such as hydroxyl, acid, ester, quinone, and ketone) indicating the presence of diverse cross-linked networks.^{49, 62} Such increased cross-linking in the OAL resins has been reported to facilitate their stronger binding to specimens.^{22, 24, 49} More systematic research is needed to clearly establish the factors contributing to the strengthening of the resins by ozonized lignin.

In a range of applied tensile stresses from 390-560 kPa, the balsa wood specimens glued with LA, OLA and combination (AL:OAL) resins experience substrate failure as evidenced by the tensile stress-strain curve [Figure S6A (SI)] and visual images of Instron-analyzed samples [Figure S7 (SI)]. However, the resins can sustain the adhesions with the surfaces (Figures 6D and 8A). A similar mode of failure for balsa wood glued with PVAc adhesive has been reported.⁶³

With CDX grade plywood (Figure 8C), maple veneer (Figure 8D) and walnut veneer (Figure 8E) samples, cohesive failure was observed with all lignin-based adhesives but in different ranges of applied tensile stresses [Figures S6B, S6C, S6D and S9 (SI)]. Cohesive failure occurs in the case of plywood at higher applied tensile stress compared to balsa wood and fiberboard. In contrast, plywood glued with PVAc and PU resins exhibits stress-strain curves characteristic of pilling type of failure (Figure S6B). Several factors, including surface interaction, mechanical interlocking between wood voids and resins, intermolecular interaction and the nature of wood multilayer composites, are known to influence the various types of failure modes.⁶⁴⁻⁶⁷ For example, the balsa wood and fiberboard specimens possess more surface roughness, are porous and in some cases have favorable surface polarity to facilitate stronger surface adhesion between the specimen and the resin.⁶⁸⁻⁷⁰ In such cases, the resins applied to balsa wood and fiberboard resins can better resist shear resulting in substrate failure at higher applied stresses. Similarly, the maple veneer (Figure 8D) and walnut veneer (Figure 8E) specimens glued with AL and OAL resins experience cohesive failure at slightly lower applied stress compared to plywood. These results show that the lignin resins can function without failure in a range of applied stresses (391 - 1127 kPa) where commercial resins have been found to be effective[Table S7, (SI)]. Maple and walnut veneers bonded with lignin resins also demonstrate cohesive failure [Figures S6C and S6D (SI)]. In contrast, substrate failure occurred in the case of veneers glued with PVAc and PU resins [Figures S6C and S6D (SI)].

For assessing the practical feasibility of the lignin-amino acid resins, we compared the performances of AL:OAL (1:1) resin (containing 50% ozone-pretreated lignin) with commercial resins (PVAc and PU) in bonding various specimens (Figure 8F). The AL:OAL (1:1) resin showed more or less similar performance as the commercial resins in bonding either balsa wood or fiberboard. The applied stresses at which substrate failure (with balsa wood, Figure 8D) or pilling (with fiberboard, Figure 8E) occurs are similar, indicating that the lignin-amino acid resins can be potential substitutes in industrial balsa wood and fiberboard applications. A similar mode of substrate failure at comparable tensile stress has been reported for balsa wood bonded with PVAc.⁶³ It must be recognized that while the PVA and PU systems are optimized commercial adhesives, the LA and OLA resins are initial unoptimized formulations.

In the case of plywood and veneer specimens (Figures 8C, 8D and 8E), the cohesive failure of the commercial resins occurs at applied stress values that are more than twofold greater than the corresponding failure values for the AL:OAL (1:1) resin. The plywood, maple, and walnut samples absorb less resin as they are less porous than balsa wood and fiberboard samples. Hence, the application of similar amounts of the resin will result in a thicker interlayer in the case of the plywood, maple and walnut samples. To understand the effect of interlayer thickness, we reduced the amount of AL:OAL (1:1) resin applied to plywood, maple, and walnut samples by half (~100 mg). The tensile strength at failure was reduced in these plywood, maple, and walnut samples by approximately 21%, 24%, and 35%, respectively (Figure S10, SI). These results provide guidance for further optimizing the properties of the LA resins, by adjusting the ozone-pretreated lignin content and other synthesis variables, to either match or outperform the commercial resins.

Based on the chemical and structural characterizations of the lignin and the resin, we suggest a plausible reaction scheme for oxidation of the lignin (Figure 9A) and the formation of the resin (Figure 9B). As shown in Figure 9A, short contact time lignin ozonolysis in a spray reactor introduces carbonyl and hydroxyl groups in the lignin.⁴¹ Similar functional groups in ozonized lignin are reported elsewhere.^{19, 22} As shown in Figure 9B, the carbonyl groups in ozonized lignin are postulated to form linkages with the amine groups in lysine in basic media.⁴⁴ The carboxylic hydroxyl group in the amino acid is not shown to be involved in crosslinking reaction based on

previous reports^{47,57} and our structural characterization results (Figure 2F) that reveal this group to be intact within the resin. This scheme provides a foundation for future detailed mechanistic studies.

SUMMARY

Lignin-amino acid-based resins were successfully synthesized in an aqueous basic medium from renewable and abundant sources (corn cob lignin and lysine) that are non-toxic. NMR (¹H, ³¹P, ¹³C-¹H HSQC, ¹⁵N-¹H HSQC and ¹⁵N-¹H HMBC) spectroscopy, FTIR spectroscopy, TGA, elemental analysis and GPC spectra reveal key structural features of the lignin-based resins including C-N cross linking and increased molar mass of the resins prepared with lignin pretreated with ozone. Qualitative vertical shear tests reveal that lignin-based resins can strongly bond pieces of wood, plastics, and metals. Against gravity, the bonded specimens can hold weights (2 kgs) that are roughly six orders of magnitude heavier than the weight of the applied resin. The bonds have endured for > 13 months thus far without breaking. Rheological measurements reveal that the tensile strengths of balsa wood and fiberboard specimens glued with lignin-amino acid resins are comparable with those reported for similar samples bonded with commercial resins such as polyurethane (PU) and polyvinyl acetate (PVAc) resins. However, the commercial resins display higher tolerance for tensile stresses than the LA resins when glued with plywood and veneer specimens. Ozone-pretreated lignin provides stronger resins offering the possibility of synthesizing optimized resins that either match or outperform the commercial resins. The lignin-amino acid resins thus show immense promise as an inexpensive and sustainable alternative for resins derived from petroleum sources. The results from this work provide guidance for future research aimed at tuning the ozonized lignin content to achieve lignin-amino acid resins with high tensile strength.

CONFLICTS OF INTEREST

The authors declare no competing financial interest.

SUPPORTING INFORMATION

TGA analyses of lignins and resins; NMR (^1H , ^{13}C , ^{31}P NMR, ^{13}C - ^1H 2D- HSQC, ^{15}N - ^1H 2D - HMBC and ^{15}N - ^1H 2D - HSQC NMR) spectroscopy of lignin and resin samples; Details of specimens used in qualitative vertical shear tests; Details of specimens used in tensile tests; Tensile stress-strain plots; Details of ozone treatment of acetosolv lignin; Pictures of balsa wood, medium density fiberboard and CDX grade plywood specimens following Instron test to assess internal bond strengths.

ACKNOWLEDGMENTS

This research was funded by a grant from the National Science Foundation Partners for Innovation Program (Award no. NSF PFI-1919267). We thank J-Six Enterprises for donating the corn cobs. We acknowledge the expertise of the University of Kansas NMR Lab in sample analysis. We acknowledge valuable technical help from the following persons at the University of Kansas. Dan Hastert for preparing the Instron samples, Sarah Ann Neuenswander and Justin Douglas, for analyzing NMR samples, Sri Charan Kakarla for running the Instron tests, Steffan Green for providing the lignin samples, Anoop Uchagawkar for helping to analyze the TGA and FTIR data, and Nakisha P. Mark for helpful discussions. We also acknowledge Kathy Lowe (Kansas State University, Manhattan, Kansas) for performing elemental analysis of the lignin samples.

REFERENCES

- (1) Conner, A. H. Wood: Adhesives. In *Encyclopedia of Materials: Science and Technology*, Buschow, K. H. J., Cahn, R. W., Flemings, M. C., Ilschner, B., Kramer, E. J., Mahajan, S., Veyssi  re, P. Eds.; Elsevier, 2001; pp 9583-9599.
- (2) Deanin, R. D.; Mead, J. L. Synthetic Resins and Plastics. In *Kent and Riegel's Handbook of Industrial Chemistry and Biotechnology*, Kent, J. A. Ed.; Springer US, 2007; pp 623-688.
- (3) Kerns, W. D.; Pavkov, K. L.; Donofrio, D. J.; Gralla, E. J.; Swenberg, J. A. Carcinogenicity of formaldehyde in rats and mice after long-term inhalation exposure. *Cancer Res* **1983**, *43* (9), 4382-4392. From NLM.
- (4) Gerberich, H. R.; Seaman, G. C. Formaldehyde. In *Kirk-Othmer Encyclopedia of Chemical Technology*, 2013; pp 1-22.
- (5) Chad Hellwinckel; Daniel De La Torre Ugarte; John L. Field; Langholtz, M. *Chapter 5: Biomass from Agriculture.* In *2023 Billion-Ton Report*; Oak Ridge National Laboratory, Oak Ridge, TN, 2024. DOI: doi: 10.23720/BT2023/2316171.
- (6) Schutyser, W.; Renders, T.; Van den Bosch, S.; Koelewijn, S. F.; Beckham, G. T.; Sels, B. F. Chemicals from lignin: an interplay of lignocellulose fractionation, depolymerisation, and upgrading. *Chem. Soc. Rev.* **2018**, *47* (3), 852-908, DOI: 10.1039/C7CS00566K.
- (7) Gong, Z.; Yang, G.; Huang, L.; Chen, L.; Luo, X.; Shuai, L. Phenol-assisted depolymerisation of condensed lignins to mono-/poly-phenols and bisphenols. *Chem. Eng. J.* **2023**, *455*, 140628. DOI: <https://doi.org/10.1016/j.cej.2022.140628>.
- (8) Bajwa, D. S.; Pourhashem, G.; Ullah, A. H.; Bajwa, S. G. A concise review of current lignin production, applications, products and their environmental impact. *Ind. Crops Prod.* **2019**, *139*, 111526. DOI: <https://doi.org/10.1016/j.indcrop.2019.111526>.
- (9) Bengtsson, A.; Bengtsson, J.; Sedin, M.; Sj  holm, E. Carbon Fibers from Lignin-Cellulose Precursors: Effect of Stabilization Conditions. *ACS Sustainable Chem. Eng.* **2019**, *7* (9), 8440-8448. DOI: 10.1021/acssuschemeng.9b00108.
- (10) Stewart, D. Lignin as a base material for materials applications: Chemistry, application and economics. *Ind. Crops Prod.* **2008**, *27* (2), 202-207. DOI: <https://doi.org/10.1016/j.indcrop.2007.07.008>.
- (11) Kalami, S.; Arefmanesh, M.; Master, E.; Nejad, M. Replacing 100% of phenol in phenolic adhesive formulations with lignin. *J. Appl. Polym. Sci.* **2017**, *134* (30), 45124. DOI: <https://doi.org/10.1002/app.45124>.
- (12) Singh, S. K.; Ostendorf, K.; Euring, M.; Zhang, K. Environmentally sustainable, high-performance lignin-derived universal adhesive. *Green Chem.* **2022**, *24* (6), 2624-2635, DOI: 10.1039/D2GC00014H.
- (13) Yang, G.; Gong, Z.; Luo, X.; Chen, L.; Shuai, L. Bonding wood with uncondensed lignins as adhesives. *Nature* **2023**, *621*, 511-515. DOI: 10.1038/s41586-023-06507-5.
- (14) Kouisni, L.; Fang, Y.; Paleologou, M.; Ahvazi, B.; Hawari, J.; Zhang, Y.; Wang, X.-M. Kraft lignin recovery and its use in the preparation of lignin-based phenol formaldehyde resins for plywood. *Cellul. Chem. Technol.* **2011**, *45*, 515-520.
- (15) Mittal, M.; Sharma, C. B. Studies on lignin-based adhesives for plywood panels. *Polym. Int.* **1992**, *29* (1), 7-8. DOI: <https://doi.org/10.1002/pi.4990290103>.

(16) Wang, S.; Yu, Y.; Di, M. Green Modification of Corn Stalk Lignin and Preparation of Environmentally Friendly Lignin-Based Wood Adhesive. *Polymers* **2018**, *10* (6), 631.

(17) Lee, Y.; von Gunten, U. Advances in predicting organic contaminant abatement during ozonation of municipal wastewater effluent: reaction kinetics, transformation products, and changes of biological effects. *Environmental Science: Water Research & Technology* **2016**, *2* (3), 421-442, DOI: 10.1039/C6EW00025H.

(18) Forni, L.; Bahnemann, D.; Hart, E. J. Mechanism of the hydroxide ion-initiated decomposition of ozone in aqueous solution. *J. Phys. Chem.* **1982**, *86* (2), 255-259. DOI: 10.1021/j100391a025.

(19) Ma, R.; Xu, Y.; Zhang, X. Catalytic Oxidation of Biorefinery Lignin to Value-added Chemicals to Support Sustainable Biofuel Production. *ChemSusChem* **2015**, *8* (1), 24-51. DOI: <https://doi.org/10.1002/cssc.201402503>.

(20) Silverman, J. R.; Danby, A. M.; Subramaniam, B. Facile Prepolymer Formation with Ozone-Pretreated Grass Lignin by In Situ Grafting of Endogenous Aromatics. *ACS Sustainable Chem. Eng.* **2020**, *8* (46), 17001-17007. DOI: 10.1021/acssuschemeng.0c03811.

(21) Lee, H.; Tomita, B.; Hosoya, S. Development of ozonized kraft lignin/epoxy resin adhesives. *Wood Indus.* **1991**, *46* (9) 412-417.

(22) Zhang, S.; Liu, T.; Hao, C.; Wang, L.; Han, J.; Liu, H.; Zhang, J. Preparation of a lignin-based vitrimer material and its potential use for recoverable adhesives. *Green Chem.* **2018**, *20* (13), 2995-3000, DOI: 10.1039/C8GC01299G.

(23) Nonaka, Y.; Tomita, B.; Hatano, Y. Viscoelastic properties of lignin/epoxy resins and their adhesive strength. *Wood Indus.* **1996**, *51* (6), 250-254.

(24) Zhang, Y.; Yan, R.; Ngo, T.-d.; Zhao, Q.; Duan, J.; Du, X.; Wang, Y.; Liu, B.; Sun, Z.; Hu, W.; et al. Ozone oxidized lignin-based polyurethane with improved properties. *Eur. Polym. J.* **2019**, *117*, 114-122. DOI: <https://doi.org/10.1016/j.eurpolymj.2019.05.006>.

(25) Bansode, A.; Portilla Villarreal, L. A.; Wang, Y.; Asafu-Adjaye, O.; Via, B. K.; Farag, R.; Vega Erramuspe, I. B.; Auad, M. L. Kraft Lignin Periodate Oxidation for Biobased Wood Panel Resins. *ACS Appl. Polym. Mater.* **2023**, *5* (6), 4118-4126. DOI: 10.1021/acsapm.3c00324.

(26) Raj, A.; Devendra, L. P.; Sukumaran, R. K. Comparative evaluation of laccase mediated oxidized and unoxidized lignin of sugarcane bagasse for the synthesis of lignin-based formaldehyde resin. *Ind. Crops Prod.* **2020**, *150*, 112385. DOI: <https://doi.org/10.1016/j.indcrop.2020.112385>.

(27) Alinejad, M.; Henry, C.; Nikafshar, S.; Gondaliya, A.; Bagheri, S.; Chen, N.; Singh, S. K.; Hodge, D. B.; Nejad, M. Lignin-Based Polyurethanes: Opportunities for Bio-Based Foams, Elastomers, Coatings and Adhesives. *Polymers* **2019**, *11* (7), 1202.

(28) Solt, P.; Konnerth, J.; Gindl-Altmutter, W.; Kantner, W.; Moser, J.; Mitter, R.; van Herwijnen, H. W. G. Technological performance of formaldehyde-free adhesive alternatives for particleboard industry. *Int. J. Adhes. Adhes.* **2019**, *94*, 99-131. DOI: <https://doi.org/10.1016/j.ijadhadh.2019.04.007>.

(29) Sarika, P. R.; Nancarrow, P.; Khansaheb, A.; Ibrahim, T. Bio-Based Alternatives to Phenol and Formaldehyde for the Production of Resins. *Polymers* **2020**, *12* (10), 2237.

(30) Zhang, Y.; Liu, Z.; Xu, Y.; Li, J.; Shi, S. Q.; Li, J.; Gao, Q. High performance and multifunctional protein-based adhesive produced via phenol-amine chemistry and mineral reinforcement

strategy inspired by arthropod cuticles. *Chem. Eng. J.* **2021**, *426*, 130852. DOI: <https://doi.org/10.1016/j.cej.2021.130852>.

(31) Pizzi, A. Wood products and Green Chemistry. *Ann. For. Sci.* **2016**, *73* (1), 185-203. DOI: [10.1007/s13595-014-0448-3](https://doi.org/10.1007/s13595-014-0448-3).

(32) Hamadi, L.; Mansouri, S.; Oulmi, K.; Kareche, A. The use of amino acids as corrosion inhibitors for metals: A review. *Egypt. J. Pet.* **2018**, *27* (4), 1157-1165. DOI: <https://doi.org/10.1016/j.ejpe.2018.04.004>.

(33) El Ibrahimi, B.; Jmiai, A.; Bazzi, L.; El Issami, S. Amino acids and their derivatives as corrosion inhibitors for metals and alloys. *Arabian J. Chem.* **2020**, *13* (1), 740-771. DOI: <https://doi.org/10.1016/j.arabjc.2017.07.013>.

(34) Boer, B.; Schneider, J.; Schoenfisch, B.; Röhm, C.; Paepke, S.; Oberlechner, E.; Ohlinger, R.; Hartkopf, A.; Brucker, S. Y.; Hahn, M.; et al. Lysine-urethane-based tissue adhesion for mastectomy—an approach to reducing the seroma rate? *Arch. Gynecol. Obstet.* **2021**, *303* (1), 181-188. DOI: [10.1007/s00404-020-05801-1](https://doi.org/10.1007/s00404-020-05801-1).

(35) Ohlinger, R.; Rutkowski, R.; Kohlmann, T.; Paepke, S.; Alwafai, Z.; Flieger, C.; Möller, S.; Lenz, F.; Zygmunt, M.; Unger, J. Impact of the Lysine-urethane Adhesive TissuGlu® on Postoperative Complications and Interventions After Drain-free Mastectomy. *Anticancer Res.* **2020**, *40* (5), 2801-2812. DOI: [10.21873/anticanres.14253](https://doi.org/10.21873/anticanres.14253).

(36) Liang, Y.; Luo, Y.; Wang, Y.; Fei, T.; Dai, L.; Zhang, D.; Ma, H.; Cai, L.; Xia, C. Effects of Lysine on the Interfacial Bonding of Epoxy Resin Cross-Linked Soy-Based Wood Adhesive. *Molecules* **2023**, *28* (3), 1391.

(37) Winblade, N. D.; Nikolic, I. D.; Hoffman, A. S.; Hubbell, J. A. Blocking Adhesion to Cell and Tissue Surfaces by the Chemisorption of a Poly-L-lysine-graft-(poly(ethylene glycol); phenylboronic acid) Copolymer. *Biomacromolecules* **2000**, *1* (4), 523-533. DOI: [10.1021/bm000040v](https://doi.org/10.1021/bm000040v).

(38) Huang, W. M.; Gibson, S. J.; Facer, P.; Gu, J.; Polak, J. M. Improved section adhesion for immunocytochemistry using high molecular weight polymers of L-lysine as a slide coating. *Histochemistry* **1983**, *77* (2), 275-279. DOI: [10.1007/bf00506570](https://doi.org/10.1007/bf00506570).

(39) Stil, A.; Liberelle, B.; Guadarrama Bello, D.; Lacomme, L.; Arpin, L.; Parent, P.; Nanci, A.; Dumont É, C.; Ould-Bachir, T.; Vanni, M. P.; et al. A simple method for poly-D-lysine coating to enhance adhesion and maturation of primary cortical neuron cultures in vitro. *Front Cell Neurosci* **2023**, *17*, 1212097. DOI: [10.3389/fncel.2023.1212097](https://doi.org/10.3389/fncel.2023.1212097).

(40) Ikeda, M. Lysine Fermentation: History and Genome Breeding. In *Amino Acid Fermentation*, Yokota, A., Ikeda, M. Eds.; Springer Japan, 2017; pp 73-102.

(41) Green, S.; Binder, T.; Hagberg, E.; Subramaniam, B. Correlation between Lignin–Carbohydrate Complex Content in Grass Lignins and Phenolic Aldehyde Production by Rapid Spray Ozonolysis. *ACS Eng. Au* **2023**, *3* (2), 84-90. DOI: [10.1021/acsengineeringau.2c00041](https://doi.org/10.1021/acsengineeringau.2c00041).

(42) Singh, S. K.; Savoy, A. W.; Yuan, Z.; Luo, H.; Stahl, S. S.; Hegg, E. L.; Hodge, D. B. Integrated Two-Stage Alkaline-Oxidative Pretreatment of Hybrid Poplar. Part 1: Impact of Alkaline Pre-Extraction Conditions on Process Performance and Lignin Properties. *Ind. Eng. Chem. Res.* **2019**, *58* (35), 15989-15999. DOI: [10.1021/acs.iecr.9b01124](https://doi.org/10.1021/acs.iecr.9b01124).

(43) Meng, X.; Crestini, C.; Ben, H.; Hao, N.; Pu, Y.; Ragauskas, A. J.; Argyropoulos, D. S. Determination of hydroxyl groups in biorefinery resources via quantitative ^{31}P NMR spectroscopy. *Nat. Protoc.* **2019**, *14* (9), 2627-2647. DOI: 10.1038/s41596-019-0191-1.

(44) Tang, J.; Mohan, T.; Verkade, J. G. Selective and Efficient Syntheses of Perhydro-1,3,5-triazine-2,4,6-triones and Carbodiimides from Isocyanates Using ZP(MeNCH₂CH₂)₃N Catalysts. *J. Org. Chem.* **1994**, *59* (17), 4931-4938. DOI: 10.1021/jo00096a041.

(45) Kihara, M.; Takayama, M.; Wariishi, H.; Tanaka, H. Determination of the carbonyl groups in native lignin utilizing Fourier transform Raman spectroscopy. *Spectrochim. Acta, Part A* **2002**, *58* (10), 2213-2221. DOI: [https://doi.org/10.1016/S1386-1425\(01\)00693-X](https://doi.org/10.1016/S1386-1425(01)00693-X).

(46) Barrera-Martínez, I.; Guzmán, N.; Peña, E.; Vázquez, T.; Cerón-Camacho, R.; Folch, J.; Honorato Salazar, J. A.; Aburto, J. Ozonolysis of alkaline lignin and sugarcane bagasse: Structural changes and their effect on saccharification. *Biomass Bioenergy* **2016**, *94*, 167-172. DOI: <https://doi.org/10.1016/j.biombioe.2016.08.010>.

(47) Yan, T.; Feringa, B. L.; Barta, K. Direct N-alkylation of unprotected amino acids with alcohols. *Sci. Adv.* **2017**, *3* (12), eaao6494. DOI: doi:10.1126/sciadv.aa06494.

(48) Kamps, J. J. A. G.; Hopkinson, R. J.; Schofield, C. J.; Claridge, T. D. W. How formaldehyde reacts with amino acids. *Commun. Chem.* **2019**, *2* (1), 126. DOI: 10.1038/s42004-019-0224-2.

(49) Shi, C.; Zhang, S.; Wang, W.; Linhardt, R. J.; Ragauskas, A. J. Preparation of Highly Reactive Lignin by Ozone Oxidation: Application as Surfactants with Antioxidant and Anti-UV Properties. *ACS Sustainable Chem. Eng.* **2020**, *8* (1), 22-28. DOI: 10.1021/acssuschemeng.9b05498.

(50) Tien, M.; Kersten, P. J.; Kirk, T. K. Selection and Improvement of Lignin-Degrading Microorganisms: Potential Strategy Based on Lignin Model-Amino Acid Adducts. *Appl. Environ. Microbiol.* **1987**, *53* (2), 242-245. DOI: doi:10.1128/aem.53.2.242-245.1987.

(51) Chatterjee, M.; Ishizaka, T.; Kawanami, H. Reductive amination of furfural to furfurylamine using aqueous ammonia solution and molecular hydrogen: an environmentally friendly approach. *Green Chem.* **2016**, *18* (2), 487-496, DOI: 10.1039/C5GC01352F.

(52) Kim, H.; Padmakshan, D.; Li, Y.; Rencoret, J.; Hatfield, R. D.; Ralph, J. Characterization and Elimination of Undesirable Protein Residues in Plant Cell Wall Materials for Enhancing Lignin Analysis by Solution-State Nuclear Magnetic Resonance Spectroscopy. *Biomacromolecules* **2017**, *18* (12), 4184-4195. DOI: 10.1021/acs.biomac.7b01223.

(53) Pinheiro, F. G. C.; Soares, A. K. L.; Santaella, S. T.; Silva, L. M. A. e.; Canuto, K. M.; Cáceres, C. A.; Rosa, M. d. F.; Feitosa, J. P. d. A.; Leitão, R. C. Optimization of the acetosolv extraction of lignin from sugarcane bagasse for phenolic resin production. *Ind. Crops Prod.* **2017**, *96*, 80-90. DOI: <https://doi.org/10.1016/j.indcrop.2016.11.029>.

(54) Diehl, B. G.; Watts, H. D.; Kubicki, J. D.; Regner, M. R.; Ralph, J.; Brown, N. R. Towards lignin-protein crosslinking: amino acid adducts of a lignin model quinone methide. *Cellulose* **2014**, *21* (3), 1395-1407. DOI: 10.1007/s10570-014-0181-y.

(55) Bule, M. V.; Gao, A. H.; Hiscox, B.; Chen, S. Structural Modification of Lignin and Characterization of Pretreated Wheat Straw by Ozonation. *J. Agric. Food Chem.* **2013**, *61* (16), 3916-3925. DOI: 10.1021/jf4001988.

(56) Figueirêdo, M. B.; Keij, F. W.; Hommes, A.; Deuss, P. J.; Venderbosch, R. H.; Yue, J.; Heeres, H. J. Efficient Depolymerization of Lignin to Biobased Chemicals Using a Two-Step

Approach Involving Ozonation in a Continuous Flow Microreactor Followed by Catalytic Hydrotreatment. *ACS Sustainable Chem. Eng.* **2019**, *7* (22), 18384-18394. DOI: 10.1021/acssuschemeng.9b04020.

(57) Chen, K.; Yuan, S.; Wang, D.; Qi, D.; Chen, F.; Qiu, X. Curcumin-loaded high internal phase emulsions stabilized with lysine modified lignin: a biological agent with high photothermal protection and antibacterial properties. *Food Funct.* **2021**, *12* (16), 7469-7479, DOI: 10.1039/D1FO00128K.

(58) Esadze, A.; Zandarashvili, L.; Iwahara, J. Effective strategy to assign ¹H-¹⁵N heteronuclear correlation NMR signals from lysine side-chain NH³⁺ groups of proteins at low temperature. *J. Biomol. NMR* **2014**, *60* (1), 23-27. DOI: 10.1007/s10858-014-9854-y.

(59) Marek, R.; Lycka, A.; Kolehmainen, E.; Sievänen, E.; Tousek, J. ¹⁵N NMR Spectroscopy in Structural Analysis: An Update (2001—2005). *Curr. Org. Chem.* **2007**, *11*, 1154-1205. DOI: 10.2174/138527207781662519.

(60) Ma, C.; Fiorin, G.; Carnevale, V.; Wang, J.; Lamb, Robert A.; Klein, Michael L.; Wu, Y.; Pinto, Lawrence H.; DeGrado, William F. Asp44 Stabilizes the Trp41 Gate of the M2 Proton Channel of Influenza A Virus. *Structure* **2013**, *21* (11), 2033-2041. DOI: 10.1016/j.str.2013.08.029.

(61) Diaz-Parga, P.; de Alba, E. Chapter Fourteen - Protein interactions of the inflammasome adapter ASC by solution NMR. In *Methods in Enzymology*, Sohn, J. Ed.; Vol. 625; Academic Press, 2019; pp 223-252.

(62) Figueirêdo, M. B.; Heeres, H. J.; Deuss, P. J. Ozone mediated depolymerization and solvolysis of technical lignins under ambient conditions in ethanol. *Sustainable Energy Fuels* **2020**, *4* (1), 265-276, DOI: 10.1039/C9SE00740G.

(63) Wu, C.; Vahedi, N.; Vassilopoulos, A. P.; Keller, T. Mechanical properties of a balsa wood veneer structural sandwich core material. *Constr. Build. Mater.* **2020**, *265*, 120193. DOI: <https://doi.org/10.1016/j.conbuildmat.2020.120193>.

(64) Mittal, K. L. The role of the interface in adhesion phenomena. *Polym. Eng. Sci.* **1977**, *17* (7), 467-473. DOI: <https://doi.org/10.1002/pen.760170709>.

(65) Browne, F. L.; Brouse, D. Nature of Adhesion between Glue and Wood1: A Criticism of the Hypothesis that the Strength of Glued Wood Joints Is Due Chiefly to Mechanical Adhesion. *Ind. Eng. Chem.* **1929**, *21* (1), 80-84. DOI: 10.1021/ie50229a023.

(66) McBain, J. W.; Hopkins, D. G. On Adhesives and Adhesive Action. *J. Phys. Chem.* **1925**, *29* (2), 188-204. DOI: 10.1021/j150248a008.

(67) Hunt, C. G.; Frihart, C. R.; Dunky, M.; Rohumaa, A. Understanding Wood Bonds—Going Beyond What Meets the Eye: A Critical Review. In *Progress in Adhesion and Adhesives*, 2019; pp 353-419.

(68) Wescott, J. M.; Birkeland, M. J.; Traska, A. E.; Frihart, C. R.; Dally, B. N. New method for rapid testing of bond strength for wood adhesives. In *30th Annual Meeting of The Adhesive Society, Inc.*, Tampa Bay, FL, February 18-21 2007, 2007; pp 219-222.

(69) Maximova, N.; Österberg, M.; Koljonen, K.; Stenius, P. Lignin adsorption on cellulose fibre surfaces: Effect on surface chemistry, surface morphology and paper strength. *Cellulose* **2001**, *8* (2), 113-125. DOI: 10.1023/A:1016721822763.

(70) Azimi, M.; Asselin, E. Improving Surface Functionality, Hydrophilicity, and Interfacial Adhesion Properties of High-Density Polyethylene with Activated Peroxides. *ACS Appl.*

Mater. Interfaces **2022**, *14* (2), 3601-3609. DOI: 10.1021/acsami.1c23703.

(71) Silverman, J. R.; Danby, A. M.; Subramaniam, B. Intensified ozonolysis of lignins in a spray reactor: insights into product yields and lignin structure. *React. Chem. Eng.* **2019**, *4* (8), 1421-1430, DOI: 10.1039/C9RE00098D.

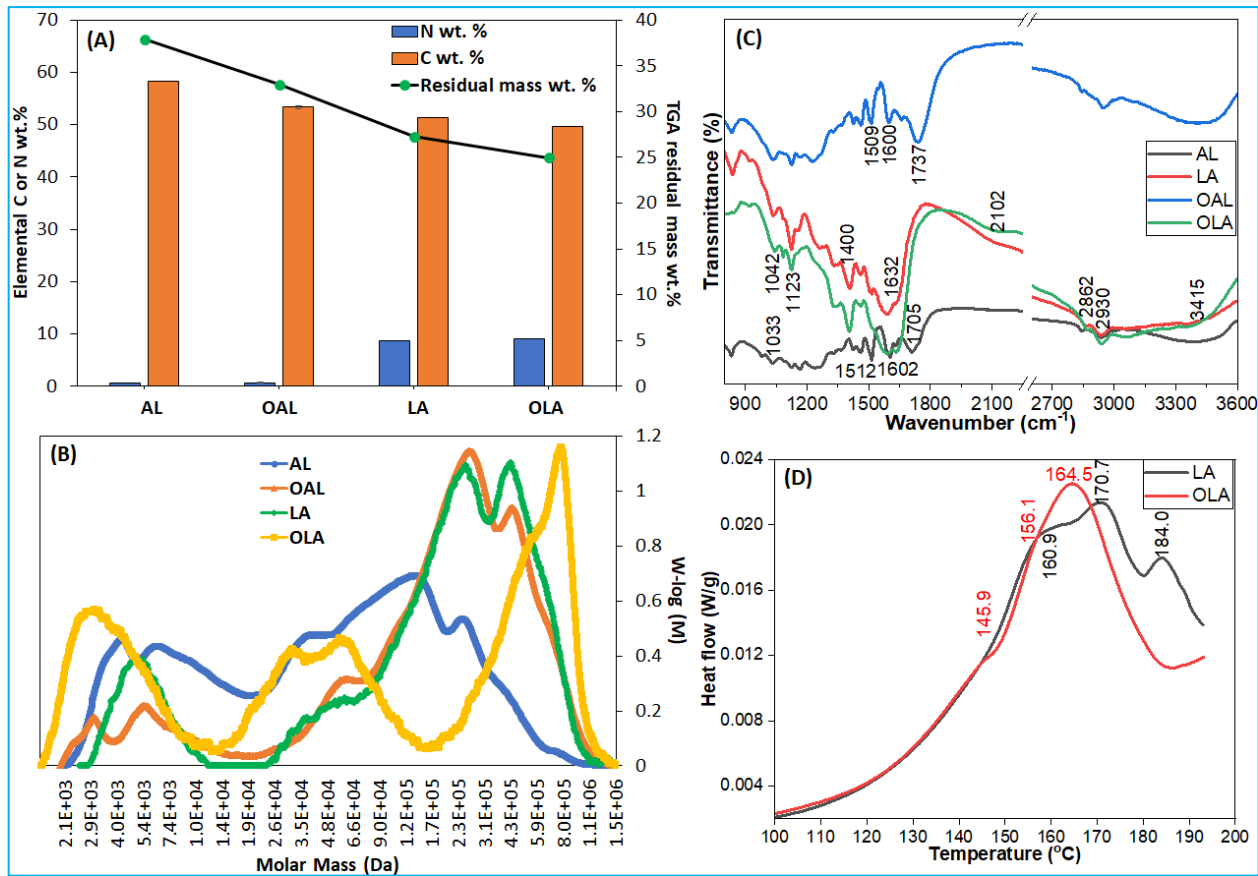


Figure 1. Physicochemical characteristics of lignins (AL and OAL) and lignin-resins (LA and OLA). (A) elemental (C, N) analyses and TGA residual mass in lignins and resins; (B) GPC chromatogram of AL, OAL, LA and OLA; (C) FT-IR spectra of acetosolv lignins (AL and OAL) and lignin-amino acid (LA and OLA) resins; and (D) DSC analysis of lignin-amino acid (LA and OLA) resins.

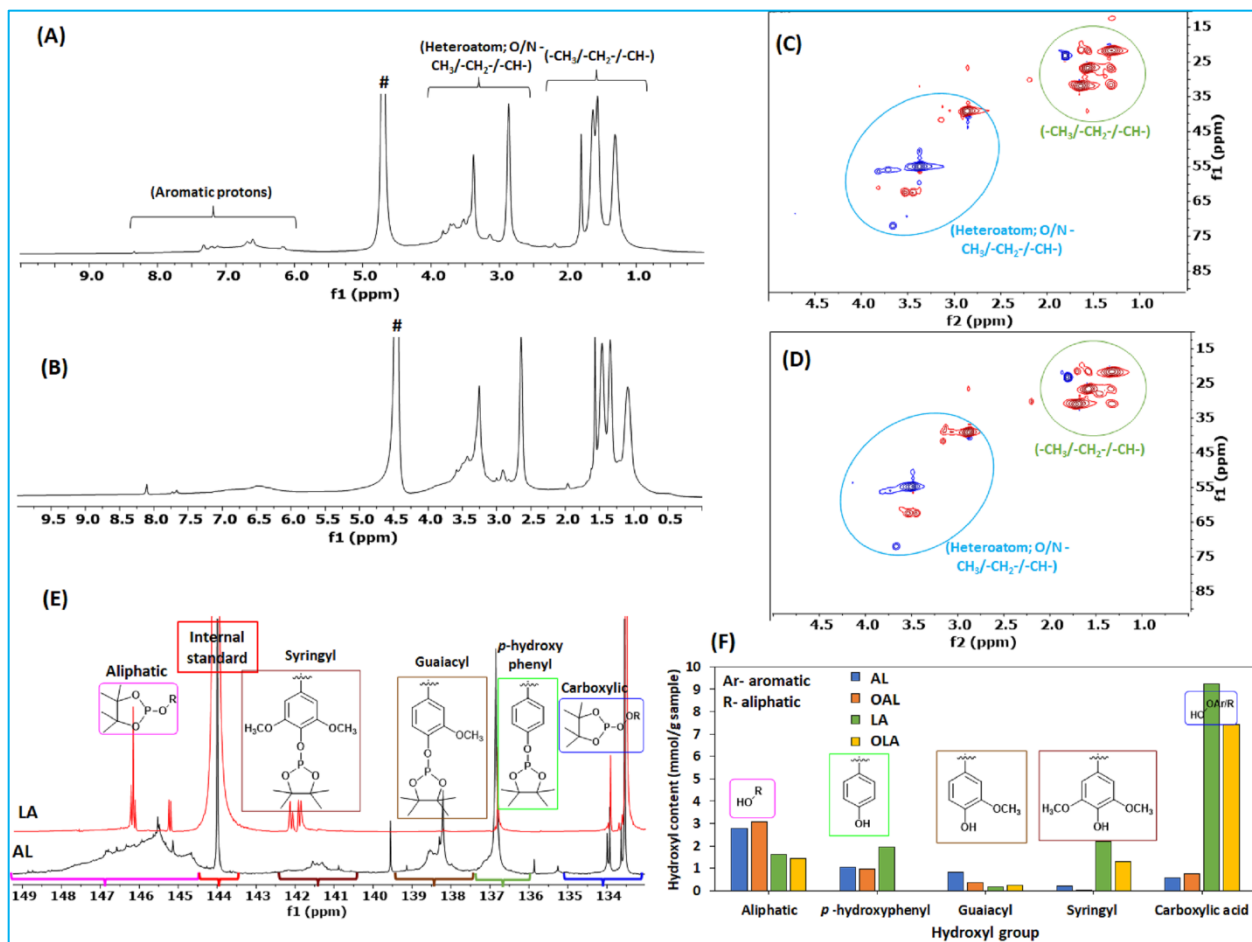


Figure 2. Insights into the structure of lignin-based resins. ^1H NMR spectra of (A) acetosolv lignin resin (LA); (B) ozonized acetosolv lignin resin (OLA). ^{13}C - ^1H -HSQC NMR spectra of (C) aliphatic region of LA; (D) aliphatic region of OLA; (E) ^{31}P NMR spectra of AL and LA; and (F) various hydroxyl groups in AL, OAL, LA and OLA determined using ^{31}P NMR. Note: peak '#' represents deuterated water.

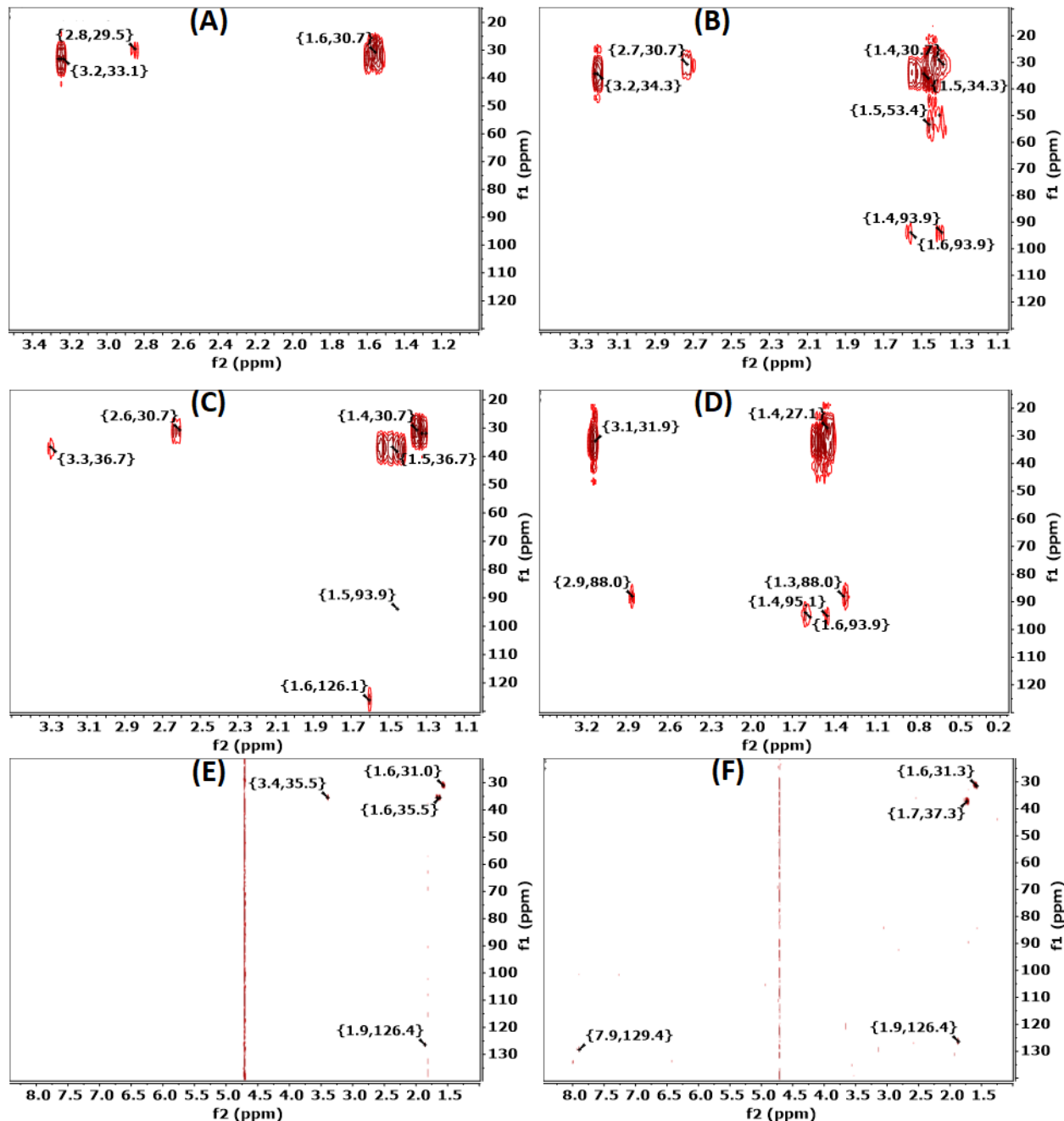


Figure 3. Structural insights into lignin-based resins using model lignin compounds. ^{15}N - ^1H HMBC NMR spectra of (A) lysine; (B) 4-hydroxy-3-methoxybenzyl alcohol and lysine formulation; (C) 4-hydroxy-3-methoxyacetophenone and lysine formulation; (D) guaiacol glyceryl ether and lysine formulation; (E) acetosolv lignin resin (LA); and (F) ozonized acetosolv lignin resin (OLA).

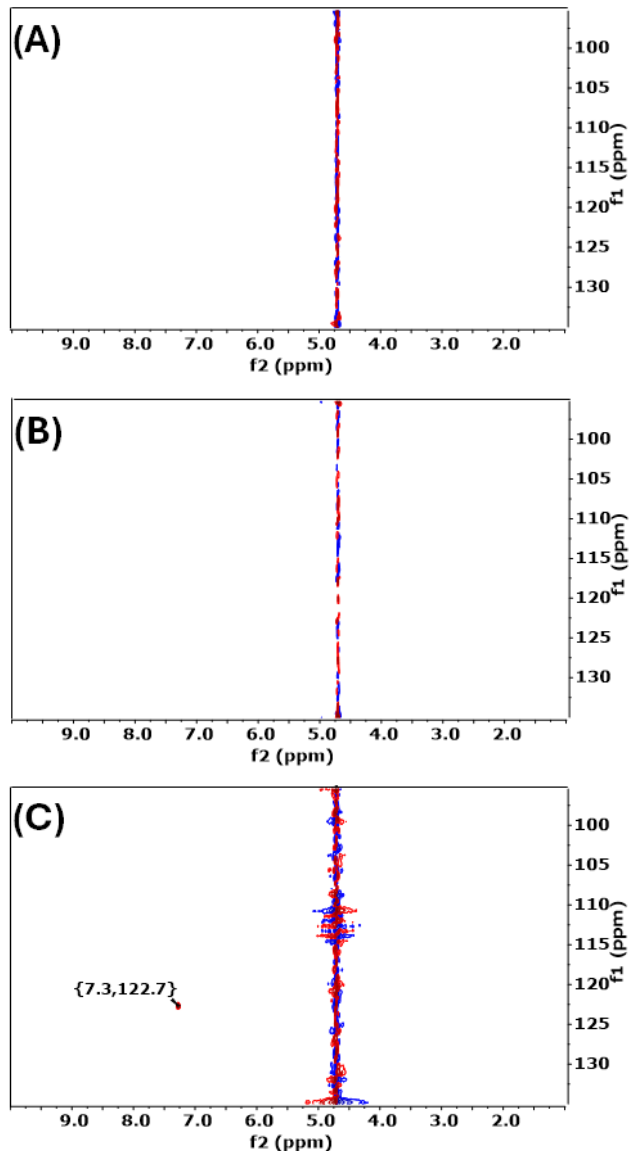


Figure 4. Structural insights into lignin-based resins. ^{15}N - ^1H HSQC NMR spectra of (A) lysine; (B) acetosolv lignin resin (LA); and (C) ozonized acetosolv lignin resin (OLA).

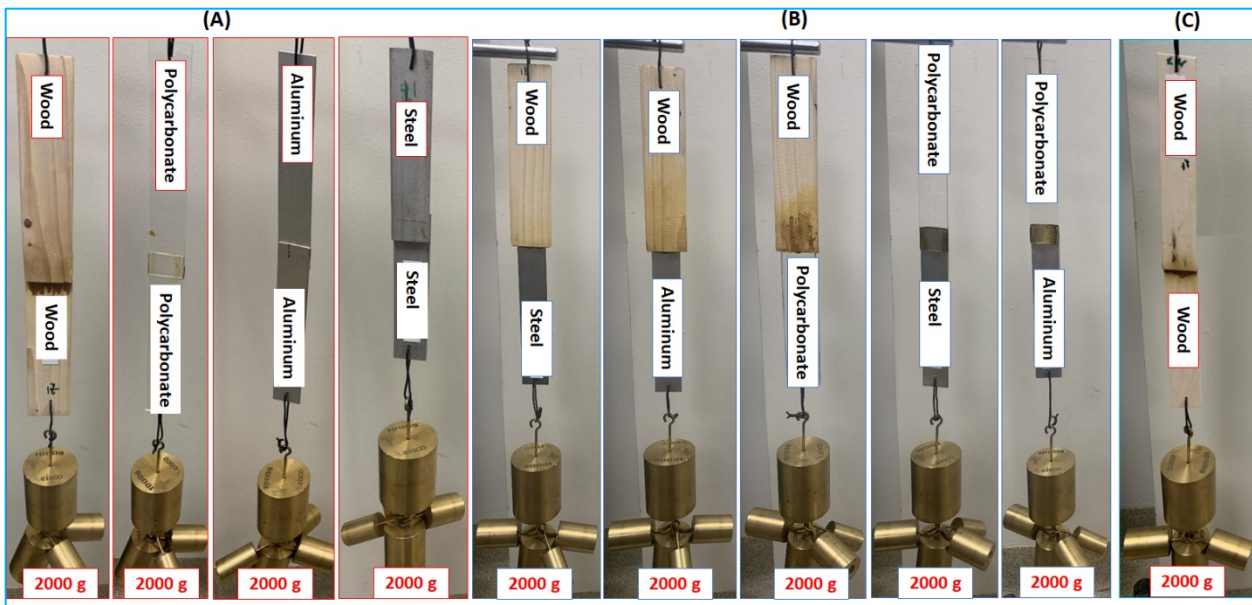


Figure 5. Qualitative vertical shear tests. (A) Homo-specimens with ozone-pretreated acetosolv lignin-lysine resin (OLA); (B) Composite-specimens with OLA; and (C) Homo-specimens with OLA have been sustaining the 2 kg loads since July 21, 2023. The tests with composite adherents commenced on October 25, 2023.

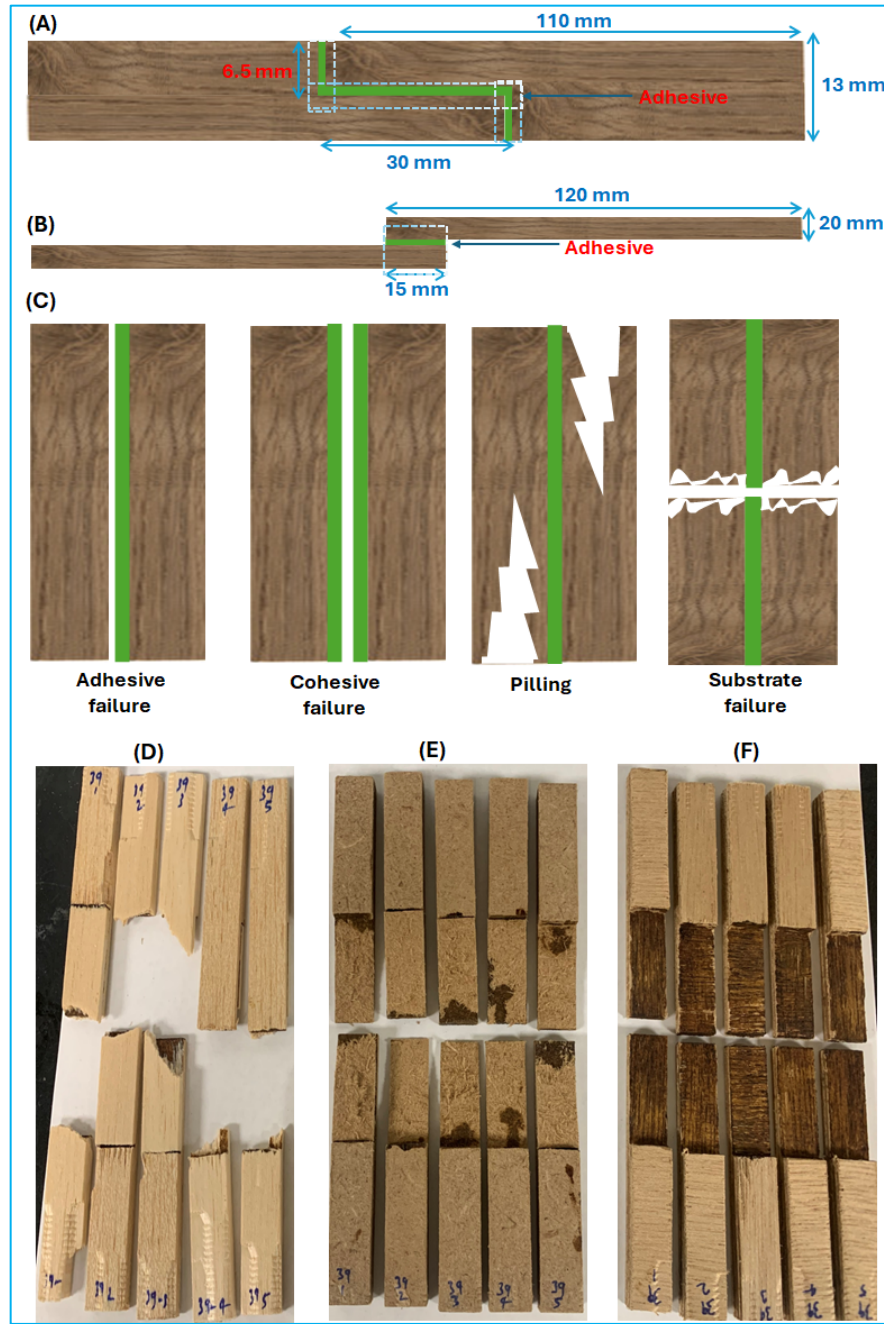


Figure 6. Schematic depiction of glued wood specimens and their images post-Instron test. (A) Schematic showing dimensions of glued wood specimens, including balsa wood, medium density fiberboard and CDX grade plywood, glued with LA, OLA, various combinations of AL:OAL resins, PVAc and PU resins; (B) Schematic showing dimensions of bonded walnut and maple veneer specimens, glued with LA, OLA, various combinations of AL:OAL resins, PVA and PU resins; (C) Types of possible failure modes during tensile stress tests: Post-Instron test images of fractures specimens from five replicate runs with (D) Balsa wood [glued with AL:OAL (1:1)]; (E) Medium density fiberboard [glued with AL:OAL (1:1)]; and (F) CDX grade plywood [glued with AL:OAL (1:1)].

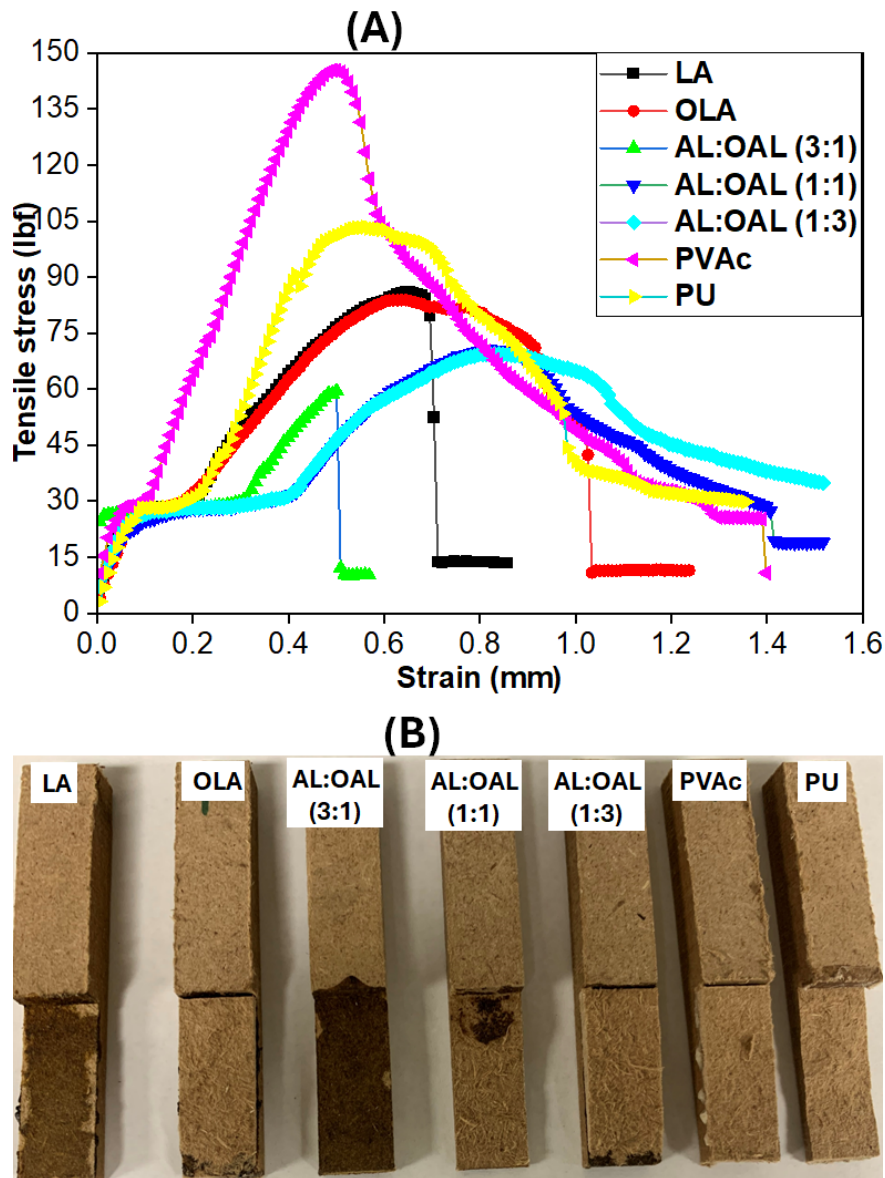


Figure 7. Structural and visual insights into specimen failure modes. (A) Instron stress-strain curves using medium density fiberboard glued with lignin and commercial resins; (B) Post Instron test images of fiberboard glued with lignin resins [LA, OLA, AL:OAL (3:1), AL:OAL (1:1), AL:OAL (1:3)], and commercial (PVAc and PU) resins.

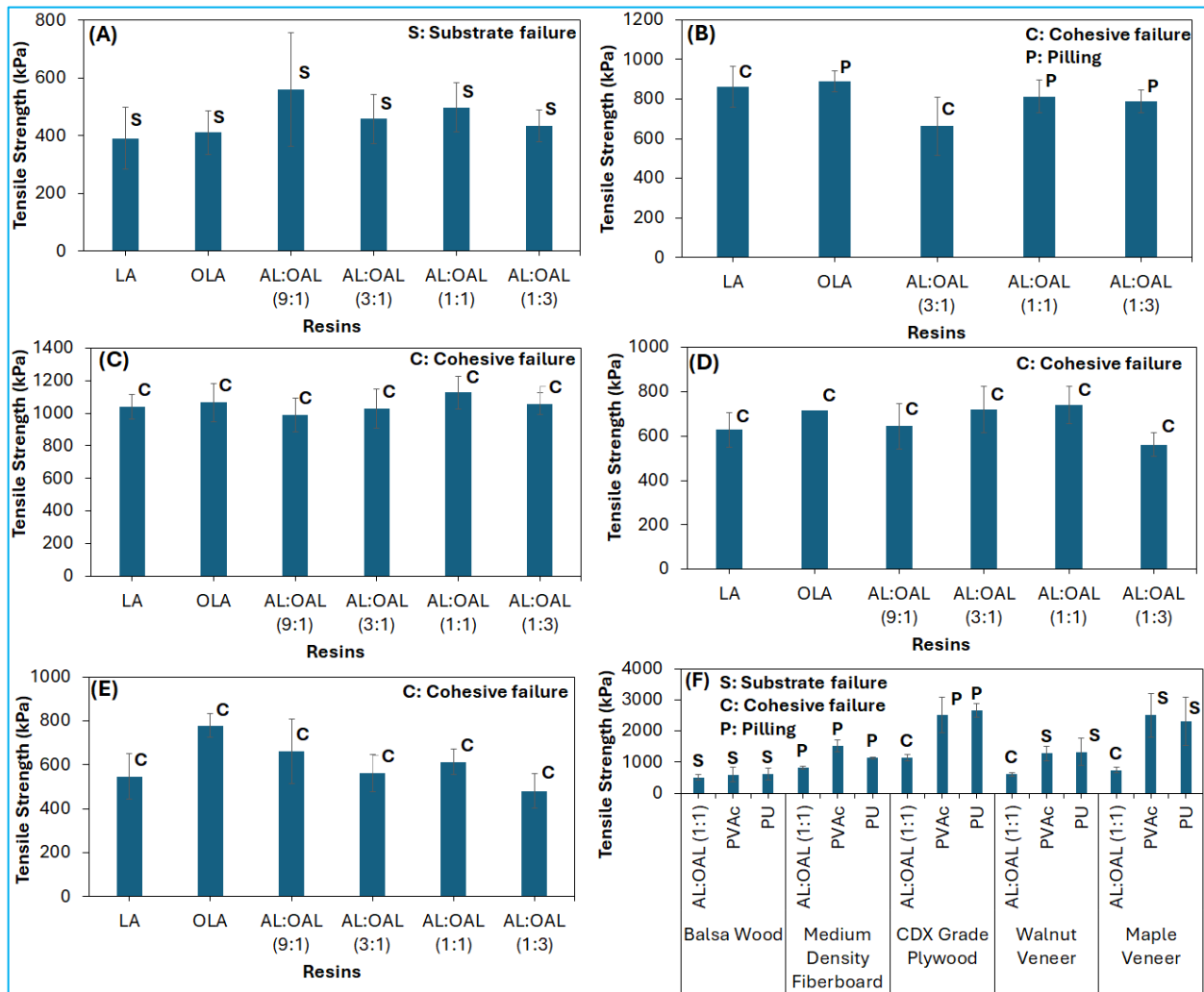


Figure 8. Comparison of mechanical performances of lignin-based and commercial resins. Tensile strengths and failure modes of various specimens glued with LA, OLA, AL:OAL (9:1), AL:OAL (3:1), AL:OAL (1:1), AL:OAL (1:3), and AL:OAL (9:1) resins; (A) Balsa wood; (B) Medium density fiberboard; (C) CDX grade plywood; (D) Maple veneer; (E) Walnut veneer, and (F) Tensile strength comparison Indicate of lignin-amino acid resin (AL:OAL, 1:1) with commercial resins (PVAc and PU) on various specimens. At least five replicates were done to assess the tensile strength of each sample. The average of these replicates is presented in Figure 8(A)-8(F), except for maple veneer glued with LA and OLA resins, for which two replicates were performed.

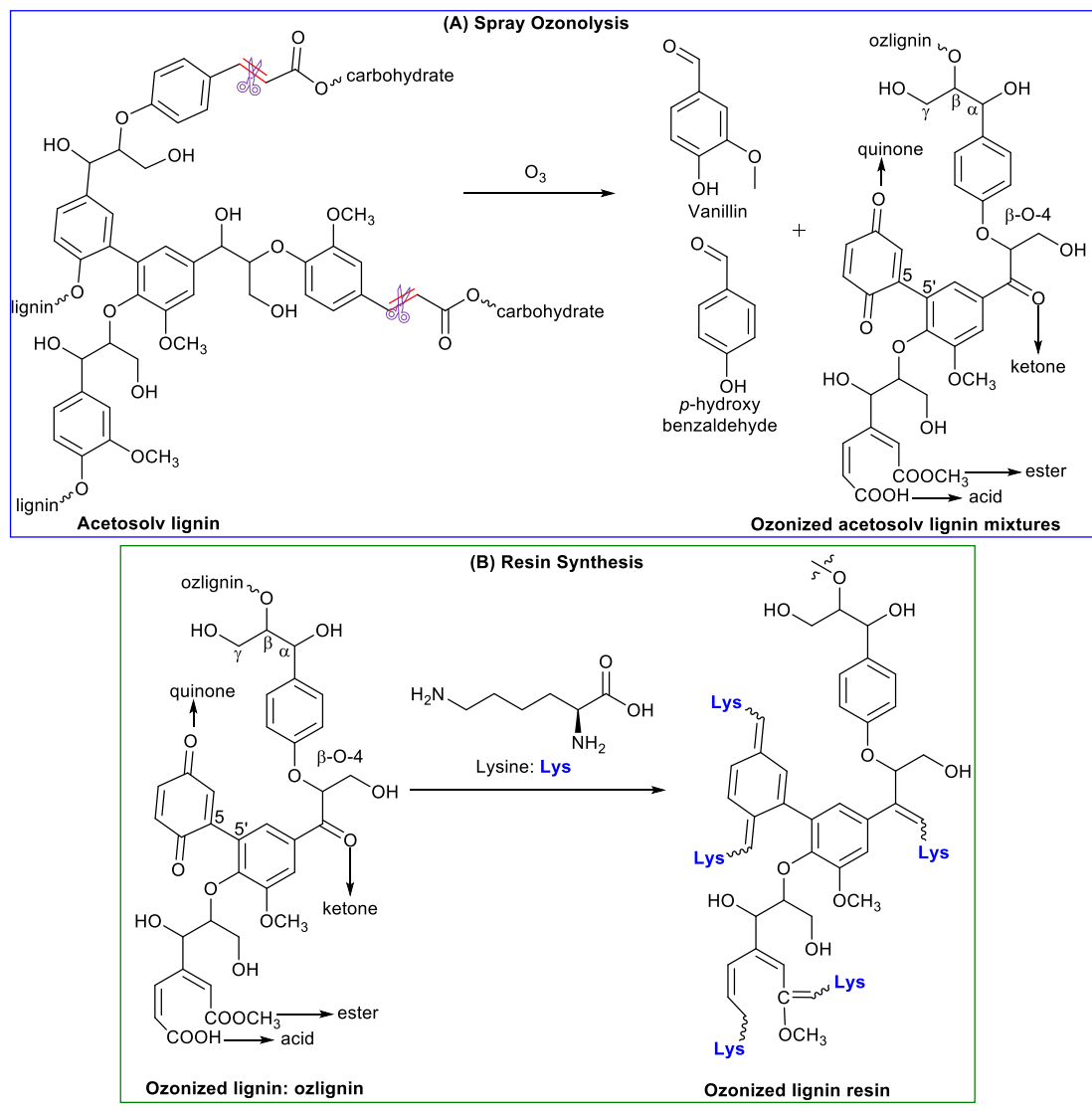


Figure 9. A proposed schematic process for lignin ozonolysis and the ozonized lignin reaction with lysine; (A) Ozonolysis of lignin; and (B) proposed reaction between ozonized lignin and lysine.^{19, 22, 49, 62, 71}